S1 Input data

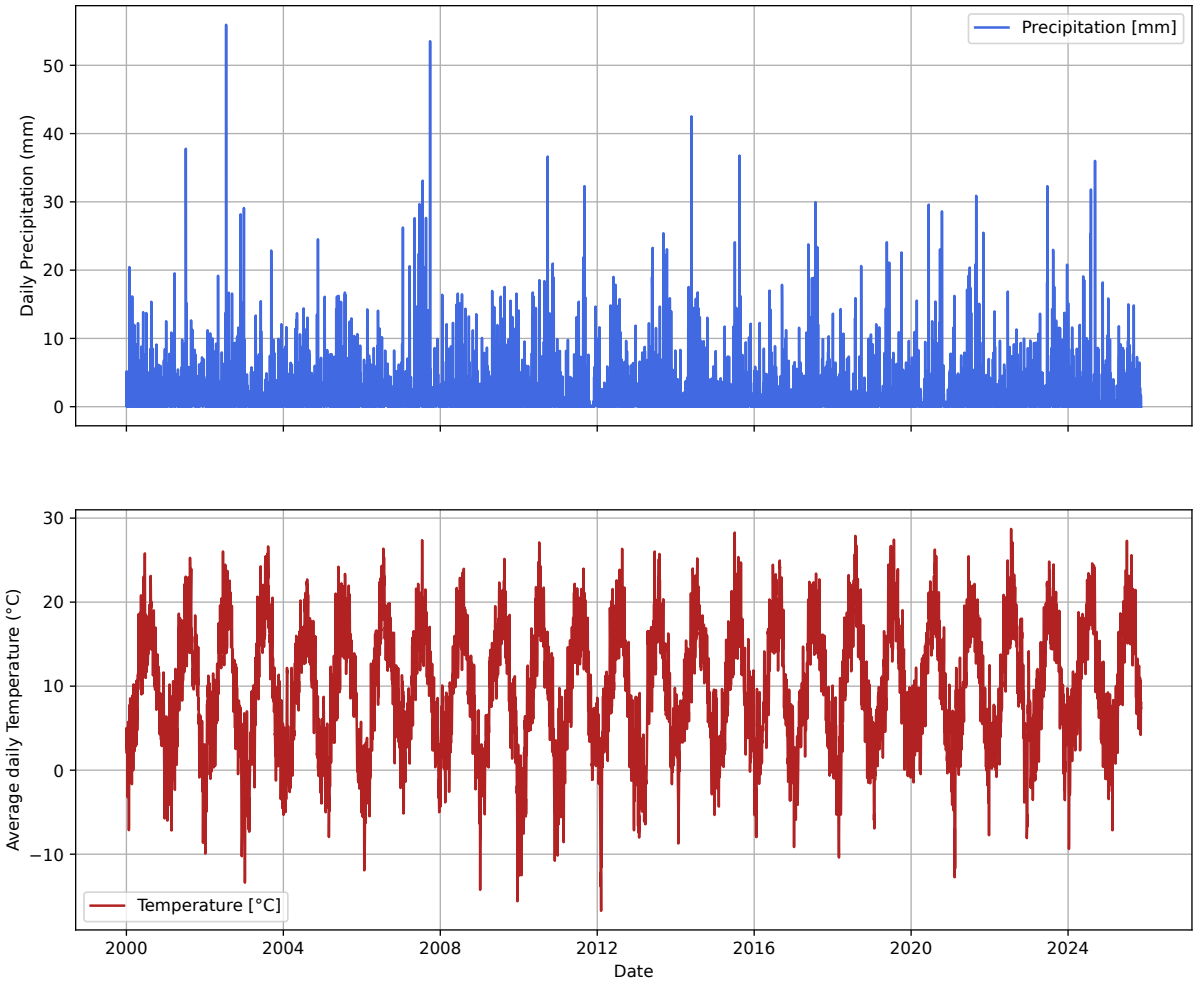

Figure S1: Daily climate input data for the Selke catchment used in model simulations.

S2 Model comparison and sensitivity test

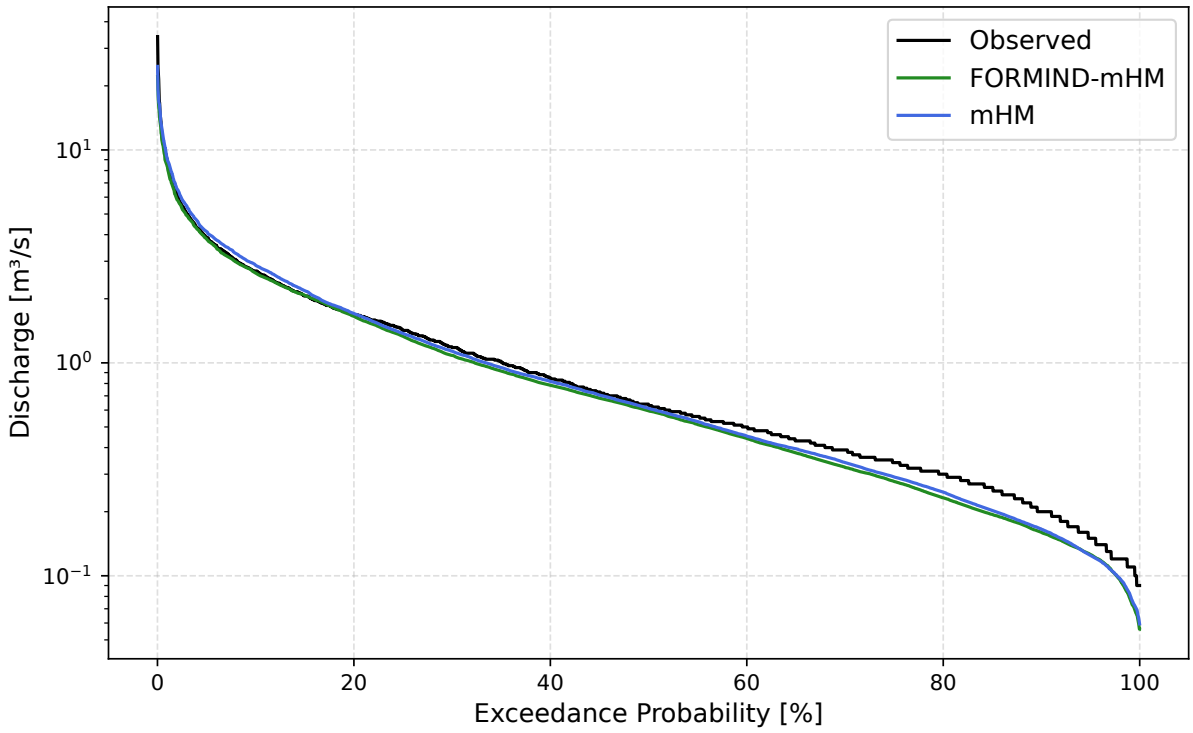

Figure S2: Flow duration curve comparing observed discharge with simulations from the coupled FORMIND-mHM framework and stand-alone mHM. Discharge [$m^3\,s^{-1}$] is plotted against exceedance probability [%] on a logarithmic y-axis.

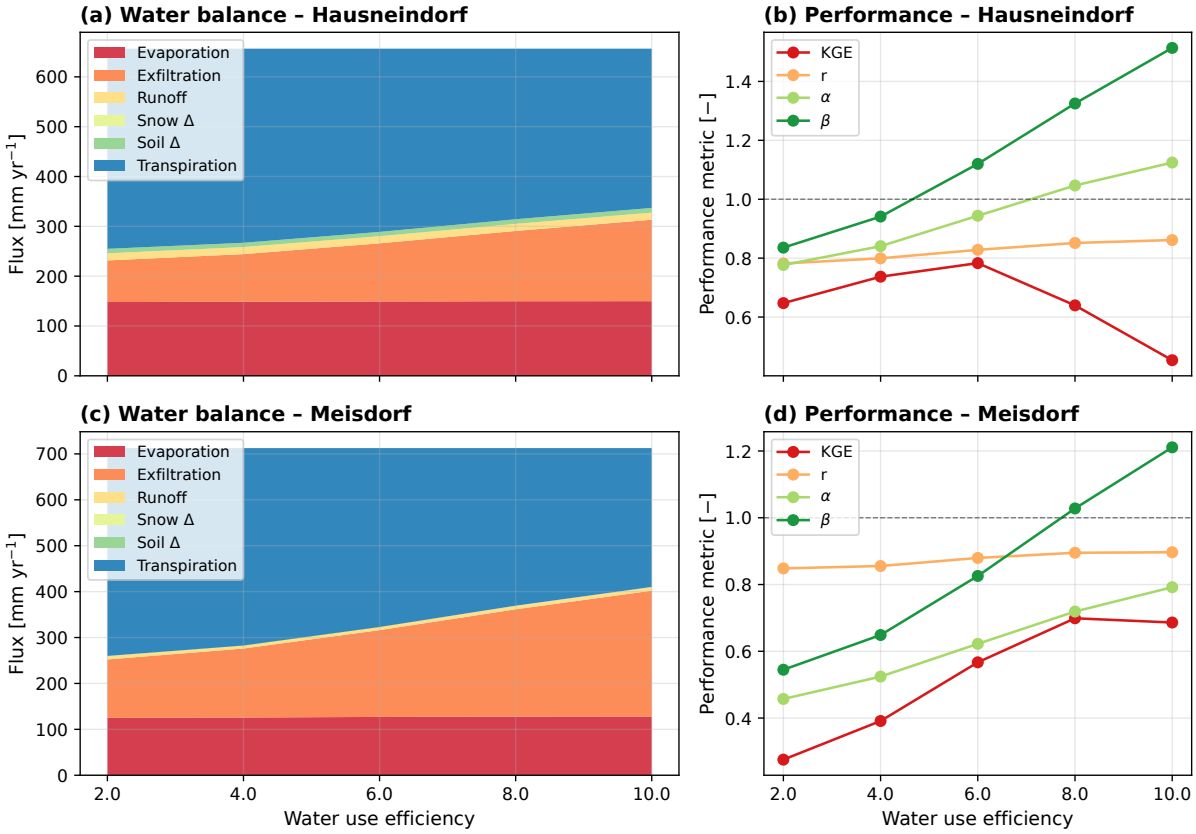

Figure S3: Sensitivity of water balance partitioning and discharge performance to water use efficiency (WUE) in FORMIND-mHM at gauges Hausneindorf (a, b) and Meisdorf (c, d). Stacked areas (a, c) show mean annual water flux components (transpiration, evaporation, exfiltration, surface runoff, snow and soil storage changes) as a function of five WUE values (2-10). Line plots (b, d) show the Kling-Gupta efficiency (KGE) and its components: correlation (r), variability ratio (α), and bias ratio (β).

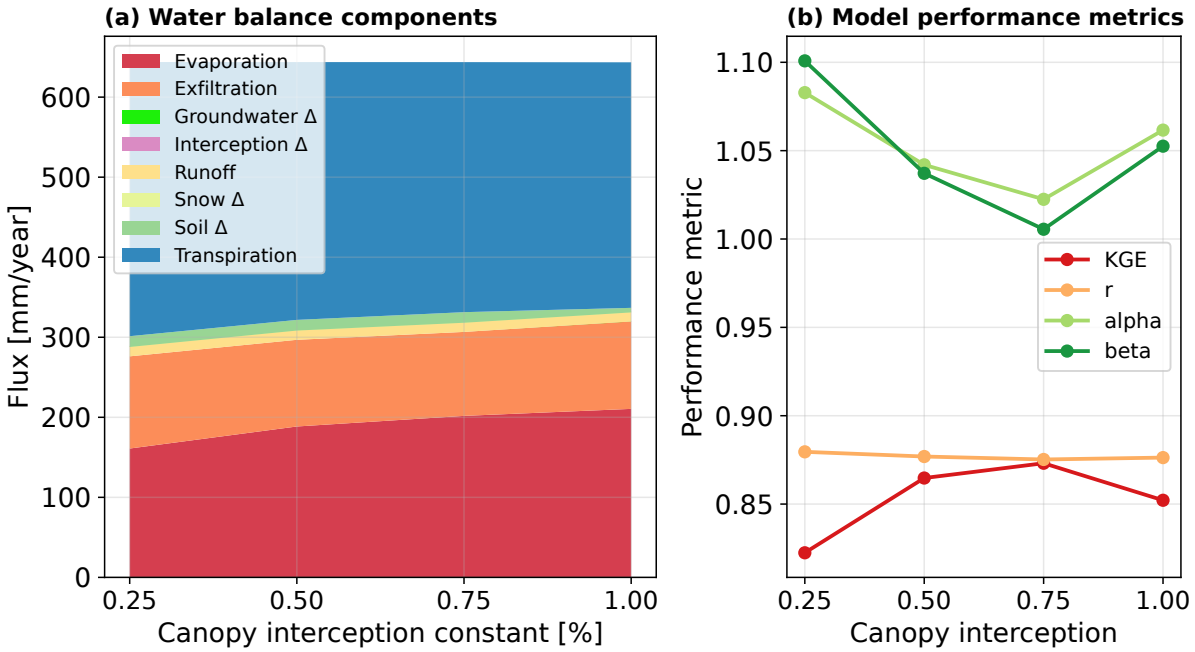

Figure S4: Sensitivity of simulated water balance partitioning and discharge performance to the canopy interception constant. Simulation runs with varying canopy interception factor for the years 2005–2015. (a) Water balance components (evaporation, exfiltration, groundwater storage change, interception storage change, runoff, snow storage change, soil storage change, and transpiration) as a function of the canopy interception constant. (b) Discharge performance metrics Kling-Gupta efficiency (KGE) and its components: correlation (r), variability ratio (α), and bias ratio (β) as a function of the canopy interception constant.

S3 Forest properties

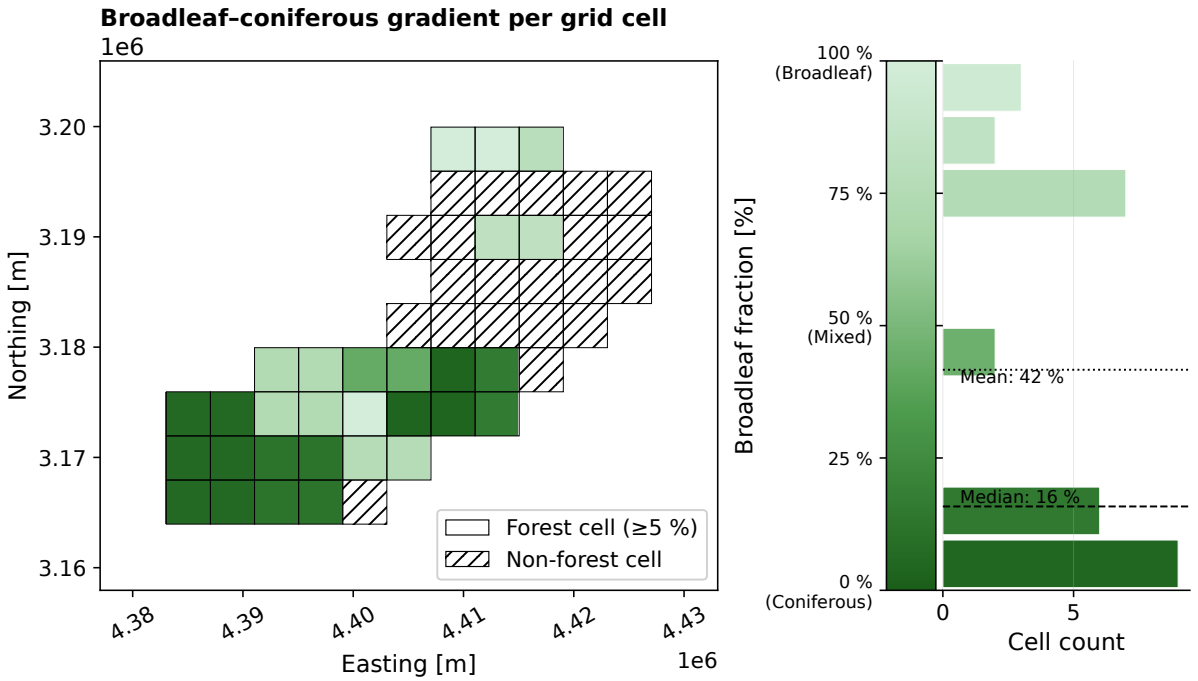

Figure S5: The map shows the tree species distribution in the Selke river catchment as represented in the coupled model framework. Broadleaf fraction per 4 km grid cell is based on tree stem counts from forest inventory data (300 × 300 m, 9 ha) assigned to each cell. The gradient ranges from conifer-dominated (0 %, dark green) to broadleaf-dominated (100 %, light green). Hatched cells indicate non-forest cover (forest fraction ≤ 5 %). The frequency distribution (right) shows the broadleaf fraction across all 29 forest cells; dashed and dotted lines indicate the median (16 %) and mean (42 %), respectively. The large difference between median and mean reflects a right-skewed distribution with a few strongly broadleaf-dominated cells in the upper catchment.

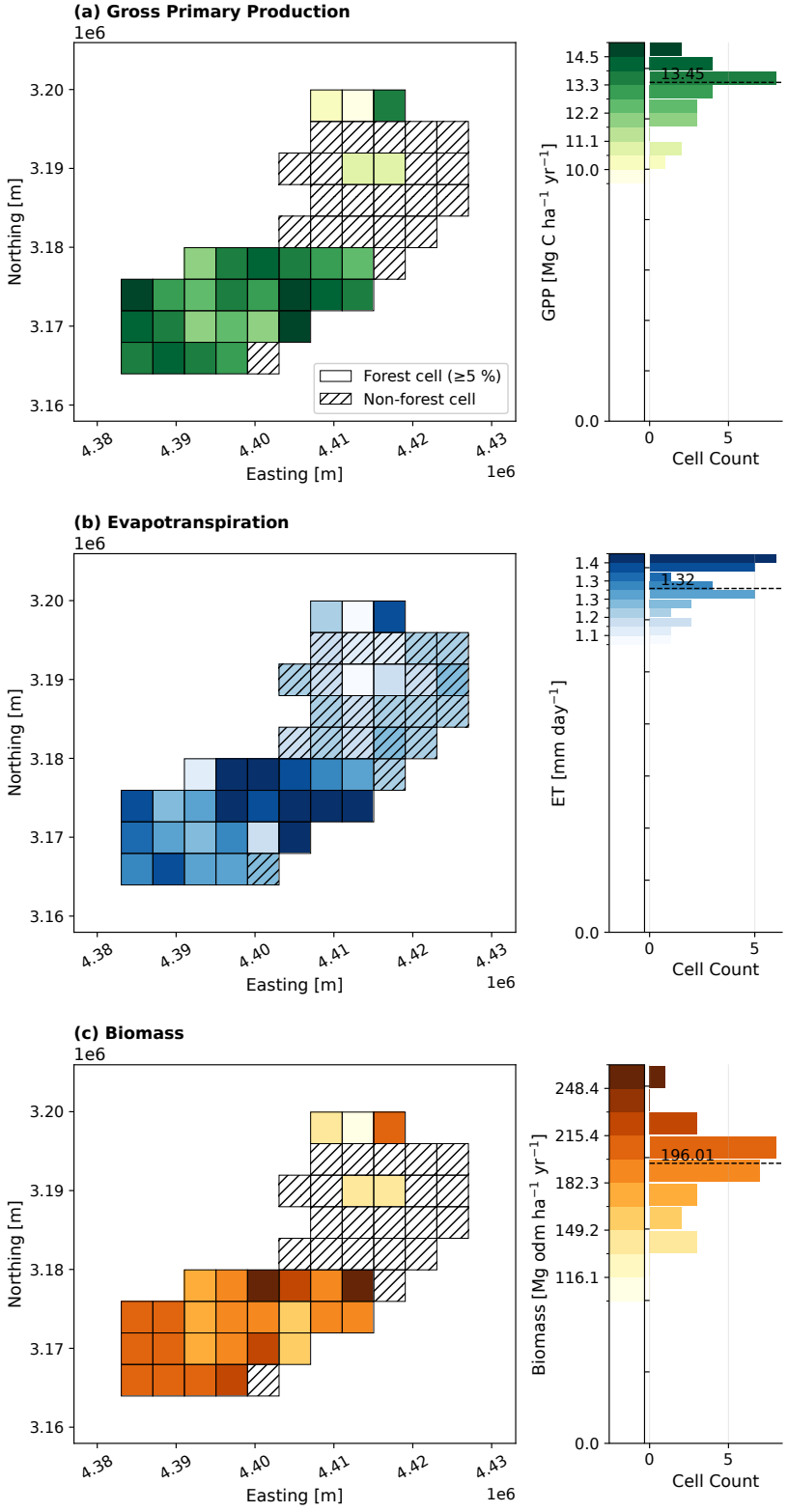

Figure S6: Mean annual spatial distribution of gross primary production (GPP), evapotranspiration (ET), and biomass increment across the Selke river catchment as simulated by FORMIND-mHM for the period 2001-2023. Colour shading shows mean annual values per 4 km grid cell for **(a)** GPP [$\mathrm{Mg\,C\,ha^{-1}\,yr^{-1}}$], **(b)** ET [$\mathrm{mm\,day^{-1}}$] as the sum of transpiration and soil evaporation, and **(c)** biomass increment [$\mathrm{Mg_{odm}\,ha^{-1}\,yr^{-1}}$]. Hatched cells indicate non-forest cover (forest fraction $< 5\,\%$). The frequency distributions (right panels) show the spatial variability across the 25 forest cells ($\geq 5\,\%$ forest fraction); dashed lines indicate the median value.

S4 Model analysis

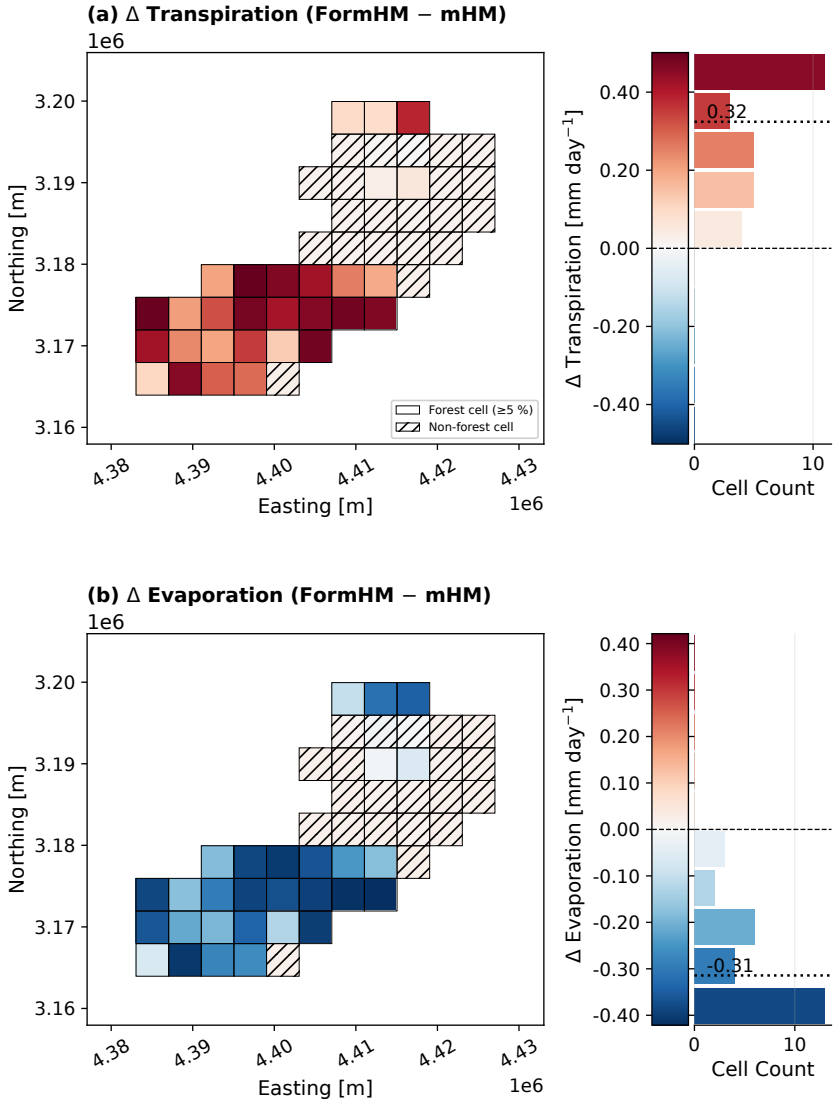

Figure S7: Difference in mean annual transpiration (**a**) and evaporation (**b**) between FORMIND-mHM and mHM (FORMIND-mHM − mHM) across the Selke river catchment, averaged over the period 2001-2023. Positive values (red) indicate higher fluxes in FORMIND-mHM, negative values (blue) indicate higher fluxes in mHM. Colour shading shows the mean daily difference per 4 km grid cell [mm day^{-1}]. Hatched cells indicate non-forest cover (forest fraction $< 5\,\%$). The frequency distributions (right panels) show the spatial variability across all 29 forest cells ($\geq 5\,\%$ forest fraction); dashed and dotted lines indicate zero and the mean difference, respectively.

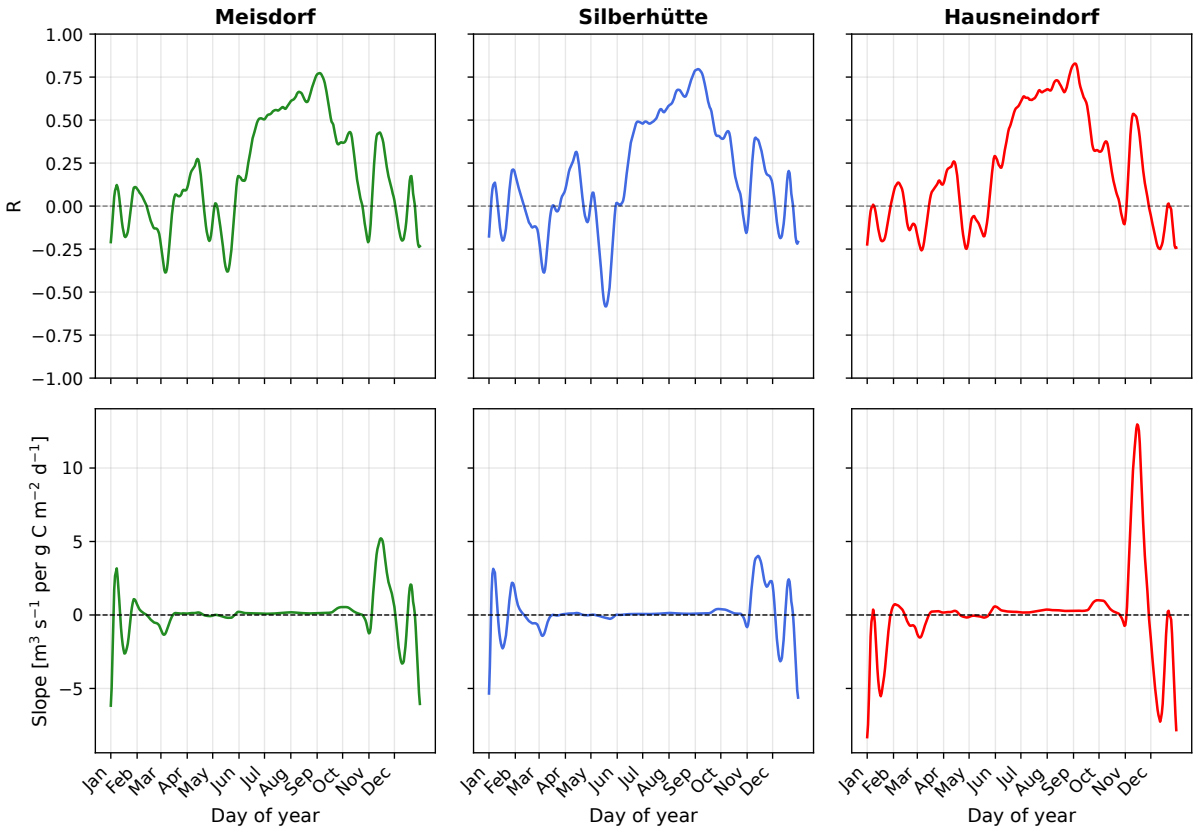

Figure S8: Seasonal relationship between simulated gross primary production (GPP) and observed discharge (Q) at gauges Meisdorf, Silberhütte, and Hausneindorf. **(Top row)** Inter-annual correlation coefficient (R) between GPP and Q as a function of day of year. **(Bottom row)** Regression slope between GPP and Q [$\mathrm{m^3\,s^{-1}}$ per $\mathrm{g\,C\,m^{-2}\,d^{-1}}$]. Both metrics are calculated using a 7-day smoothing window, a lag of 15 days, and a day-of-year window of ± 7 days.